COBEM 2023 27TH INTERNATIONAL CONGRESS OF MECHANICAL ENGENEERING

ABCM Brazilian Society of Mechanical Sciences and Engineering
27th ABCM International Congress of Mechanical Engineering
December 04-08, 2023, Florianópolis-SC, Brazil

COBEM-2023-0779 – EXPERIMENTAL STUDY IN AN OPTICALLY ACCESSIBLE SPARK IGNITION ENGINE USING METHANE IGNITION WITH A LATERAL SPARK PLUG UNDER STOICHIOMETRIC AND LEAN COMBUSTION

Enrico Rapetti Malheiro de Oliveira*
Fábio Dias
Alexander Penaranda
Leila Ribeiro dos Santos
André Luiz Martelli
Pedro T. Lacava
Aeronautics Institute of Technology (ITA), Laboratory of Combustion, Propulsion and Energy, São José dos Campos, SP, Brazil.
*enrico.oliveira@ga.ita.br.

Abstract. *Commonly, in-cylinder pressure and exhaust gas analyses are used to investigate spark-ignition engines, but they lack details about the combustion process. To gain deeper insights into combustion itself, several authors have increasingly used optical techniques. In this study, it was employed optical methods to investigate combustion flame propagation in a unique setup where the spark plug is positioned laterally, which promotes ignition and flame propagation near the cylinder wall. This approach leads to greater heat exchange with the wall than with the center of the combustion chamber, where further investigation is needed to compare these results with engine cyclic variability, flame stability, and wrinkling. Experiments were conducted using methane (CH_4) as fuel under stoichiometric and lean conditions at a fixed engine speed of 1000 rpm. The fuel mass flow rate was varied to adjust the air-fuel ratio (λ) to 1.5. The results revealed non-uniform flame propagation speeds, flame front stretching, and wrinkling due to the lateral spark plug positioning, resulting in engine instabilities and cyclic variability. Also, increasing air dilution resulted in less stable and efficient combustion. Leaner mixtures showed slower flame development and lower NO emissions.*

Keywords: *Experiments in optical access engine, Flame images processing, Lateral ignition, Methane gas, Lean combustion.*

1. INTRODUCTION

Internal combustion engines are typically evaluated based on in-cylinder pressure data, which provide a general understanding of engine performance without revealing the underlying phenomena. To gain a deeper understanding of the combustion process, optical techniques are used to gain access to the flame in optically accessible engines. Optical studies provide valuable insights into combustion development and can serve as diagnostic tools in the product development phase (Malheiro de Oliveira *et al.*, 2022; Henrique Rufino *et al.*, 2023; Martinez *et al.*, 2017; Aleiferis and Behringer, 2015; Aleiferis *et al.*, 2010, 2013; Augoye and Aleiferis, 2014; Di Iorio *et al.*, 2016). Research engines with optical accessibility allow either the implementation of complicated optical diagnostic techniques or the retention of full engine functionality while accommodating diagnostic requirements. However, the modifications required for optical techniques may affect the behavior of a commercial engine (Winklhofer, 2001).

Direct observation of the flame through the piston window is a commonly used optical technique that, in conjunction with appropriate image post-processing techniques, allows calculation of the parameters associated with flame growth (Malheiro de Oliveira *et al.*, 2022; Henrique Rufino *et al.*, 2023; Martinez *et al.*, 2017). Cycle-based imaging provides insight into the ignition process, flame front propagation, and the late combustion phase. The integration of thermodynamic and optical investigations thus aims at analyzing the combustion process itself.

In this study, the positioning of the spark plug was changed to the lateral side. As a result, the ignition and part of the flame now propagate in the immediate vicinity of the cylinder wall, resulting in a higher heat exchange with the wall than in the case of the flame portions propagating toward the central area of the chamber. This discrepancy in heat transfer results in different rates of flame front propagation, which in turn causes stretching and wrinkling effects. These effects can lead to instabilities and cyclic fluctuations in the system.

Experiments were conducted in an optically accessible spark ignition engine, in which the cylinder head of the GSE-T4 1.3L engine (from Stellantis) was integrated into the optical research engine. Methane was used with this engine configuration to evaluate the functionality of these devices under the effects on engine stability, performance, flame morphology, and exhaust emissions. Air dilutions under stoichiometric and lean conditions were used, and test conditions were set at 1000 rpm, with constant air mass flow and variable fuel mass flow. The air-fuel ratio (λ) was increased up to

a value of 1.5.

2. EXPERIMENTAL PROCEDURE

To perform the experimental tests, the apparatus includes an AVL 5406 spark ignition engine with optical access, active AC dynamometer, fuel injection line, port-fuel injector (PFI), high-speed camera with an intensifier, data acquisition system, and control units, Figure 1. The research engine was adapted using the cylinder head from the GSE-T4 1.3L engine (Otto cycle) from Stellantis (Former PSA and Fiat), which gave a compression ratio of 6.6 with the optical liner. Detailed engine specifications are not disclosed due to confidentiality concerns.

The camera acquisition consisted of a high-speed phantom VEO1310 camera coupled with a HiCATT 23 S20 100ns (High-speed Intensified Camera Attachment) intensifier from Lambert Instruments. Together with the camera and intensifier, the optical setup uses a UV-Nikon 105mm f/4.5 lens attached. Optical access to the combustion chamber was ensured by a fused silica window (65mm diameter) fixed on the piston crown and a 45° UV-enhanced mirror in the bottom of the elongated piston. The specific set-up allows 79% coverage of the entire cross-section of the cylinder bore cross-sectional area. Figure 1 also shows from the optical access the combustion chamber geometry, indicating the intake and exhaust valves, spark plug, and pressure transducer. The spatial resolution for this experiment was 97.2 μm / pixel, and the exposure time was equivalent to one CAD. For all optical measurements, the crank-angle encoder signal synchronized the camera and the engine through a delay unit. The crank angle reference was made to the TDC at the end of compression.

In this study, the spark plug is placed on the side of the cylinder due to a cylinder head adjustment, as shown in Figure 1. The spark plug position causes the flame to exchange heat with the wall first, which compromises the flame's development. Therefore, the flame front propagates at different speeds; causing stretching and wrinkling that can lead to instabilities and cyclic variability.

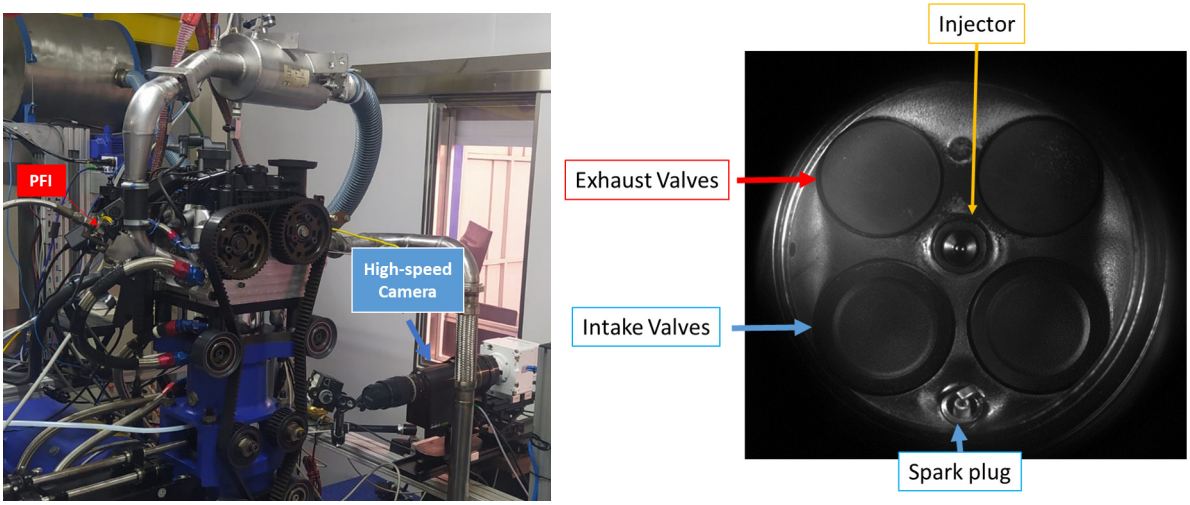

Figure 1. (Left) Representation of the experimental engine arrangement. (Right) Combustion Chamber geometry, with the intake and exhaust valves, spark plug, pressure transducer and direct injector.

The engine's speed was set at a constant 1000 rpm to investigate lean-burn combustion under conditions of low turbulence and low engine operating speeds, using port-fuel injection (PFI) fueling with methane gas. The PFI injection pressure was consistently maintained at 6 bar. All timing references are provided in terms of "Crank Angle Degree" (CAD), with 1 CAD equivalent to 0.167 ms at the 1000 rpm speed employed throughout this study. Table 1 outlines the operational parameters used to achieve lean combustion with methane. To ensure a meaningful study comparison, the duration of injection (DOI in milliseconds) was adjusted to attain the desired air-fuel ratio (λ). An accuracy of ±1% is maintained by the Bosch LSU 4.9 wideband oxygen sensor positioned in the exhaust port, which measures air dilution. Consequently, the air-fuel ratio is determined based on the wideband sensor signal, and this determination is compensated for according to the type of fuel used by the ETAS ES630 module. It is necessary to input the hydrogen-to-carbon (H/C) and oxygen-to-carbon (O/C) ratios, along with the stoichiometric air/fuel ratio when needed.

The performance and stability of the engine were evaluated through the indicated mean effective pressure (IMEP) and related Coefficient of Variation (CoV_{IMEP}) (Heywood, 1988). The ignition timing, SOI, and air mass flow, m_{air}, was fixed in all conditions. In this study, the λ was set at stoichiometric conditions and it was increased by 0.1 until the λ at 1.5.

The image post-processing procedure was developed by the authors (Malheiro de Oliveira *et al.*, 2022; Henrique Rufino *et al.*, 2023) to obtain a detailed analysis of flame morphology (Ozdor *et al.*, 1994) using a routine script developed in the software MATLAB. For the routine script, the first step was to use the acquired 8-bits images to be treated to retrieve the

Table 1. Operation parameters from the combustion of methane (CH_4) at stoichiometric and lean conditions at 1000 rpm.

Ignition timing (°CA)	$\dot{m}_{air}$ (kg/h)	**SOI** (°CA)	**DOI** (°CA)
-15	8.14	240	Varied to reach the desired λ

flame front geometric parameters (Original Image, Figure 2-a). After extracting the intensity level, a circular mask was fixed on the spark plug to cut off the light from the reflections at the optical access limits (Figure 2-b). Next, the procedure adjusts the contrast and brightness of the images concerning the maximum intensity value to optimize the signal-to-noise ratio. The next step is to apply a threshold (Otsu, 1979) to obtain binary images with the value 1 (red) associated with a pixel that corresponds to the object and 0 (black) for the background of the image. And then, make morphological transformations to fill holes and remove small objects that are not part of the flame and can mask the evaluation of the morphological parameters (Figure 2-c). And with this, it is possible to retrieve the flame curvature and other parameters to proper analyze flame wrinkling, distortion, circularity and other parameters.

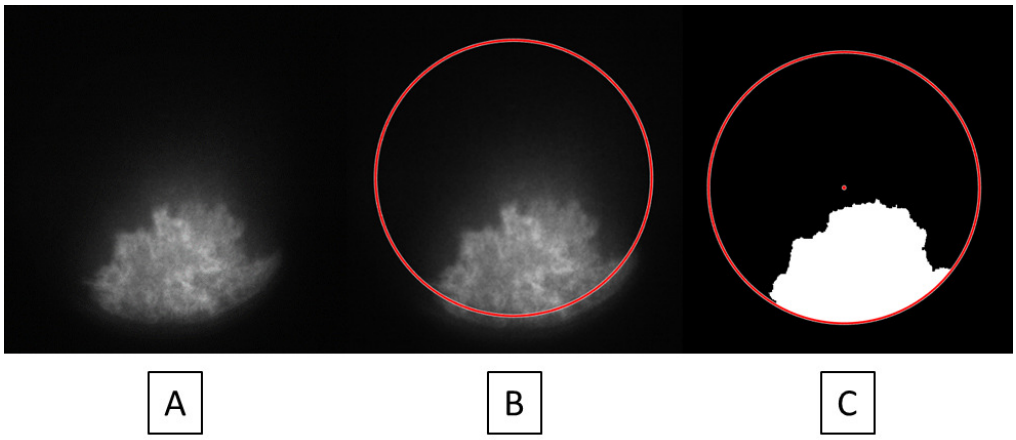

Figure 2. Script developed for image processing using MATLAB.

In this study, the spark plug is placed on the side of the cylinder due to a cylinder head adjustment, as shown in Fig. 1. This placement causes the flame to exchange heat with the wall first, which compromises the flame's development. Therefore, the flame front propagates at different speeds; causing stretching and wrinkling that can lead to instabilities and cyclic variability. For this reason, the study aims to investigate the flame propagation speed in different directions from the spark plug to examine the influence of the flame igniting near the wall on its development, Fig. 3, to identify the flame speed in 7 different directions using the Eq. 1 below.

$$S_d\,(N) = \frac{d_{(i+1)} - d_{(i)}}{\Delta t}, \tag{1}$$

where N is the direction fixed from the spark plug, $S_d\,(N)$ is the flame propagation speed in N, $\Delta t(x)$ is the time between frames (or for the period indicated), and d_i is the distance between the spark plug and the last point that intersects the line N, which it is the distance between two points ($d_{AB} = \sqrt{(X_b - X_a)^2 + (Y_b - Y_a)^2}$, as A$(X_a, Y_a)$ and B(X_b, Y_b)). Using this methodology, it is possible to identify the patterns from the flame development, which can understand how the flame propagates, as shown in the example with methane in Fig. 3 with their flame distance. It should be emphasized that our calculations of flame propagation speed were limited to the optical access region where the increase in the flame area follows a linear trend. This suggests that any variations in speed within this range are negligible (Malheiro de Oliveira *et al.*, 2022). Further study will be necessary to compare these results with engine cyclic variability, flame stability, and wrinkling.

The gaseous emissions species concentrations (CO, THC, and NOx) were measured in the undiluted exhaust gas stream using a Multigas 2030 spectrometer analyzer (MKS Instruments). The equipment work with the Fourier Transform Infrared (FTIR) principle that is capable for acquiring multiple gas species with one test sample for a second on parts per billion (ppb) to parts per million (ppm) sensitivity. Gas hose heater maintains temperature before the sample enters the gas cell and the equipment provides automatic temperature and pressure compensation to ensure accurate analysis. The resolution was 1 ppm for CO and 0.5 ppm for the other three chemical species, all within 5% equipment accuracy. In addition, the O_2 concentration was measured using a NOx lambda probe sensor at the outlet of the MKS equipment, which measures NOx emissions and oxygen concentration. Oxidant dilution correction was set it at 3% as normally used for spark-ignition engines.

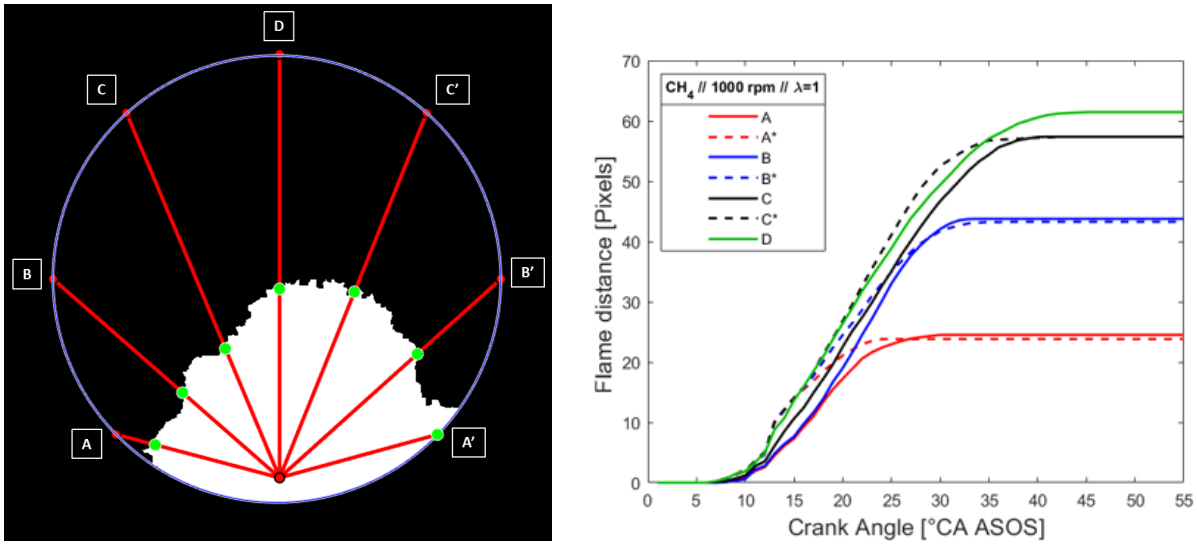

Figure 3. (Left) Identification of flame propagation distance through seven directions. (Right) Mean flame distances analyzed in seven directions (A, A', B, B', C, C', and D) at 1000 rpm, $\lambda = 1$, with CH_4 through 40 cycles.

3. RESULTS AND DISCUSSION

Table 2 shows the thermodynamic results obtained from an average of 100 consecutive cycles varying the air-fuel ratio from stoichiometric conditions (λ=1.0) to λ=1.5. Since the ignition timing was kept constant, it is possible to analyze the combustion at the specified angle of 10% of the mass fraction burned (AI10) and 50% of the mass fraction burned (AI50). It can be observed that combustion takes significantly longer when the engine is operated with leaner mixtures. The performance parameters, such as IMEP (Indicated Mean Effective Pressure) and CoV$_{IMEP}$ (Coefficient of variation of IMEP), are shown below. A better IMEP is obtained with a stoichiometric mixture, while leaner mixtures lead to a deterioration of the performance. In addition, a higher oxidizer concentration leads to more unstable operation, as shown by the increased CoV$_{IMEP}$.

Table 2. Thermodynamic results for the combustion of methane (CH_4) at stoichiometric and lean conditions at 1000 rpm..

Air-Fuel Ratio (λ) -	**O2** [%]	**IMEP** bar	**CoV**$_{IMEP}$ %	$\lambda_{Measured}$ -	**AI10** °CA	**AI50** °CA
1.0	0.843	3.07	1.44	1.01	7.09	16.46
1.1	2.545	3.03	1.60	1.10	7.93	17.79
1.2	3.617	2.89	1.43	1.18	9.23	19.92
1.3	4.649	2.71	2.10	1.27	11.73	23.78
1.4	6.028	2.49	4.21	1.38	16.33	31.15
1.5	7.718	1.56	40.17	1.56	29.11	53.15

The thermodynamic analysis is based on the pressure measured in the cylinder, which results from the combination of the piston motion and the energy released during the combustion reactions. Figure 4 shows in-cylinder pressure curves for methane at stoichiometric to lean mixtures. The pressure curves are averages of the last 50 consecutive cycles.

Figure 4 depicts the in-cylinder pressure curves and ROHR profiles for methane. Peak pressure decreased for leaner mixtures due to less efficient combustion. Consequently, as mentioned in the optical analyses, the temperature decreases due to the higher air-fuel ratio, resulting in slower flame development, which is one of the factors explaining the higher CCV and combustion instability. However, from a point where the mass of inert gases absorbs a lot of energy and the flame propagation speed decreases significantly, much more energy is later released (in the final stages of combustion) as can be seen in leaner mixtures with higher CoV$_{IMEP}$. Complementing with integral heat release in Fig. 5, the energy released is way more efficient delivered with stoichiometric mixtures than lean mixtures.

In the context of extreme lean conditions, it was observed that the variability of the cycle, as indicated by the coefficient of variation of indicated mean effective pressure (CoV_{IMEP}), exhibited significant fluctuations. Specifically, for an air-fuel equivalence ratio (λ) of 1.4, the CoV_{IMEP} displayed a fluctuation of approximately 4.21%, whereas, for λ = 1.5, the variability increased drastically to around 40.17%. These values signify unstable engine operations and occasionally result in misleading indications regarding the observed trend as the combustion becomes leaner. Consequently, it is important to acknowledge that extreme conditions beyond 5% are present in the results; however, they are not considered reliable

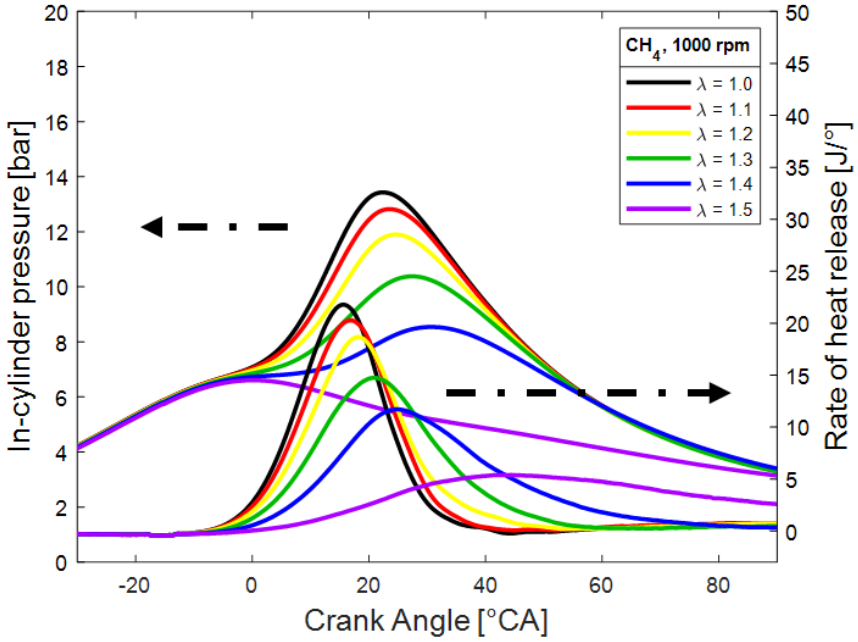

Figure 4. (Left) In-cylinder pressure and (Right) ROHR for methane at 1000 rpm using stoichiometric to lean mixtures.

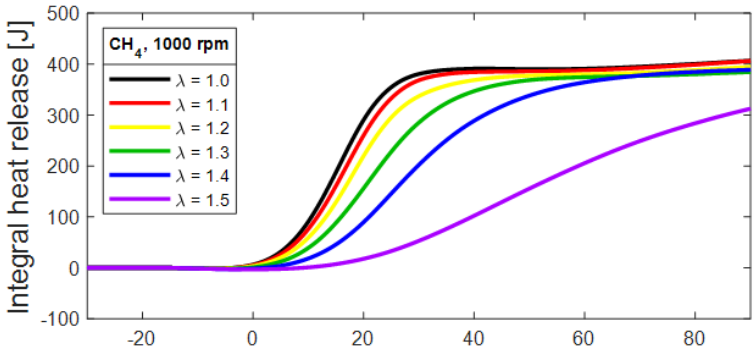

Figure 5. Integral heat release for methane at 1000 rpm using stoichiometric to lean mixtures.

for drawing definitive conclusions or identifying trends.

To visually illustrate this phenomenon, Fig. 6 presents a sequence of images depicting methane combustion across stoichiometric to lean conditions. Notably, the brightness of the flames diminishes as the air-to-fuel ratio increases, which signifies incomplete combustion. Furthermore, the flame front becomes increasingly unstable and exhibits a wrinkled appearance as the mixture becomes leaner, as shown in Fig. 7, which showcases the mean flame curvature obtained over 40 cycles. This observation aligns with the findings obtained from the thermodynamic data. As the air-fuel mixture becomes more leaner, the challenges associated with flame propagation become more pronounced. Consequently, the flame propagation speed decreases, resulting in instabilities and cyclic variations. For an air-fuel ratio of λ = 1.5, the CoV_{IMEP} surpasses 40%. This level of instability is characterized by misfire cycles and incomplete combustion. Even when considering that the data is derived from mean images obtained over 40 cycles, the propagation of flame curvature does not occur as intended. More importantly, what it is possible to note is that when the combustion becomes leaner, it tends to develop more through the direction of the combustion chamber center. This is explained by the heat exchanges interactions of the flame first with the wall, impairing the development of the flame though its vicinity.

Figure 8 presents the flame speed propagation based on an average of 40 consecutive cycles of images, it was compared the tests conducted with stoichiometric and lean combustion across seven propagation lines originating from the lateral spark plug. By placing the spark plug in a lateral position, the ignition and certain parts of the flame tend to propagate closer to the cylinder wall. This results in greater heat exchange with the wall compared to the portions of the flame that spread towards the center of the chamber. As depicted in Fig. 8, the flame speed propagation for λ=1 is higher than that observed in lean mixtures in all directions. As the temperature decreases with lean mixtures, the flame propagation speed decreases, with a greater influence observed in direction D, towards the center of the cylinder. Nevertheless, as shown in

Fig. 7, the flame initially propagates towards the center of the cylinder along lines C, C*, and D before spreading closer to the walls as the mixture becomes leaner.

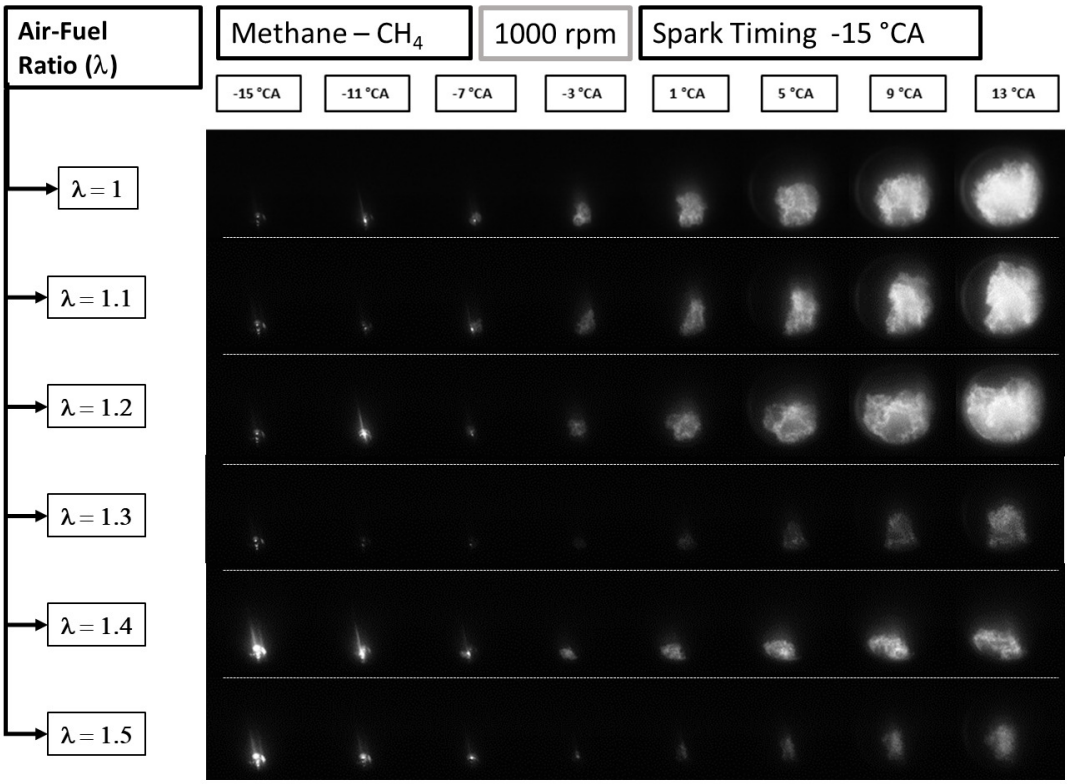

Figure 6. Flame front evolution through the crank angle degrees for λ=1.0 to λ=1.5.

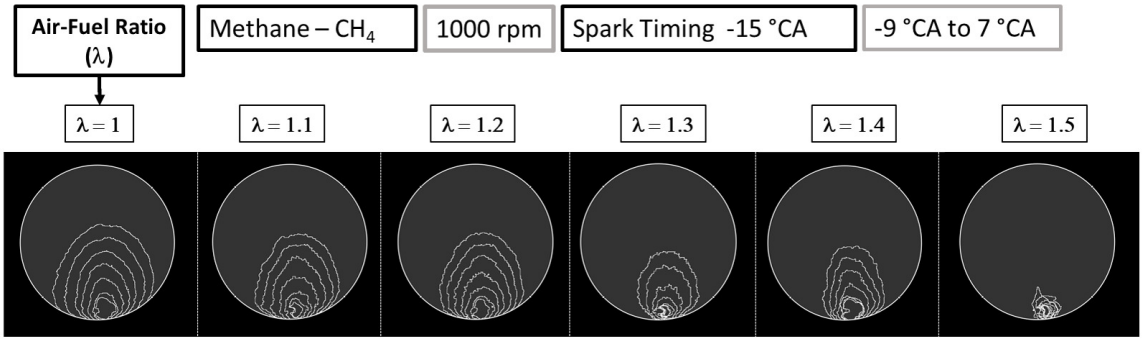

Figure 7. Flame front curvature for λ=1 to λ=1.5 through mean images of 40 cycles from -9 °CA to 7 °CA.

Table 3 presents a comparison of CO, NOx, and THC levels for methane combustion at various air-fuel ratios, considering $\lambda = 1$. As the air-fuel ratio increases, it is observed that NOx emissions increase up to 1.1 and then decrease to 1.5. This behavior can be attributed to Zeldovich's mechanism of NO formation, which states that NO production is directly proportional to the higher temperatures present in the air-fuel mixture. Therefore, with leaner combustion, the temperature of the mixture decreases, resulting in reduced NO formation (Malheiro de Oliveira *et al.*, 2022).

When analyzing CO and THC emissions, several factors should be taken into account. Firstly, the engine operates at lower temperatures in a thermal transient regime compared to a commercial engine. Additionally, the optical engine exhibits a larger crevice between the piston and cylinder. Consequently, the sealing rings are positioned lower, allowing the flame to propagate into this volume, thereby increasing the heat exchange surfaces between the flame and the cylinder/piston surfaces (Solferini de Carvalho *et al.*, 2022; Irimescu *et al.*, 2013). The presence of larger crevice volumes in the engine leads to the accumulation of more residual fuel, and/or an excessively fuel-rich mixture with incomplete combustion results in the formation of THC (Kim *et al.*, 2017). Hence, lean combustion tends to have a higher concentration of THC since a significant portion of CH_4 remains unburned. Regarding CO emissions, higher concentrations

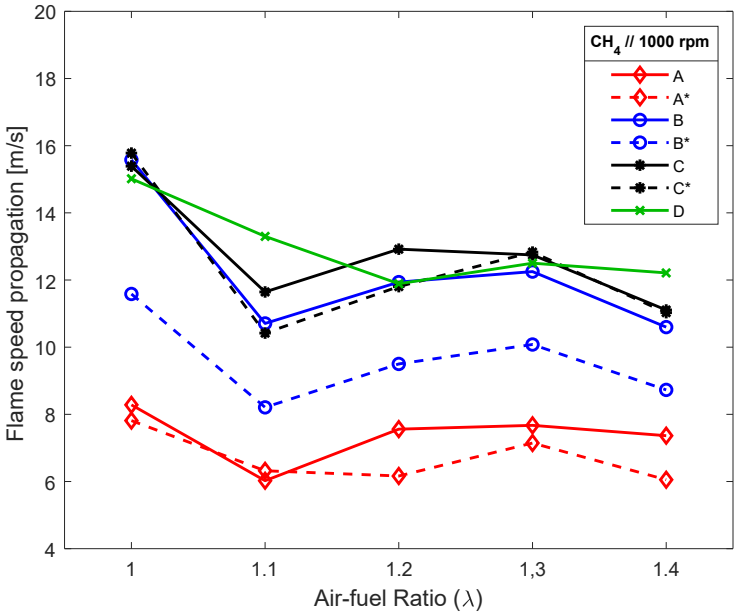

Figure 8. Average flame speed propagation of stoichiometric to lean combustion through the 7 lines of propagation from the lateral spark plug.

are achieved under stoichiometric conditions, while lean combustion yields almost the same concentration values. Typically, CO formation occurs due to insufficient oxygen, and with lean combustion, the availability of oxidant in the air-fuel mixture reduces, resulting in lower CO formation.

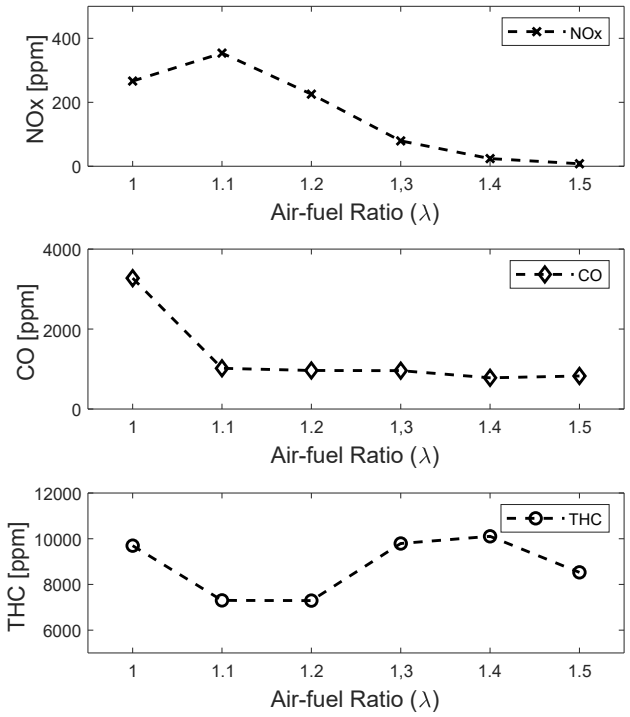

Figure 9. Exhaust emissions for NO_x, CO, and THC for methane at 1000 rpm using stoichiometric to lean mixtures.

Table 3. Comparison of CO, NOx, and THC levels at different air-fuel ratios with $\lambda = 1$ for methane combustion.

Air - fuel Ratio (λ)	CO	NOx	THC
1.0	-	-	-
1.1	-69%	33%	-25%
1.2	-71%	-15%	-25%
1.3	-71%	-70%	1%
1.4	-76%	-91%	4%
1.5	-75%	-97%	-12%

4. CONCLUSIONS/REMARKS

The present paper investigated the effects of laterally placing the spark plug in an internal combustion engine on flame propagation speed, instabilities, and cyclic variability. The study employed optical techniques and image post-processing to analyze the combustion process and its correlation with thermodynamic parameters and exhaust emissions.

The experimental results revealed that the lateral placement of the spark plug led to non-uniform flame propagation speeds, stretching, and wrinkling of the flame front. These factors contributed to instabilities and cyclic variability in engine operation. The research engine utilized in the study allowed for optical access and maintained full engine operability, providing valuable insights into the evolution of combustion. The post-processing of images facilitated the calculation of flame growth parameters and the identification of flame propagation patterns.

The study also examined the impact of different air-fuel ratios on combustion performance, indicating that leaner mixtures resulted in longer combustion development times, decreased performance, and increased instability. The observed decrease in flame propagation speed with lean mixtures was more pronounced towards the center of the cylinder. Overall, these findings emphasize the importance of considering flame propagation characteristics and their interaction with the cylinder wall to optimize engine performance and stability. Further investigations are necessary to explore the relationship between flame propagation, cyclic variability, flame stability, and wrinkling.

From a thermodynamic perspective, it was observed that increasing air dilution results in more unstable and less efficient combustion. With leaner mixtures, as temperatures decrease, the flame exhibits slower development and NO emissions also decrease. Furthermore, the AI50 mixture demonstrated a slower flame speed compared to other air-fuel mixtures. Additionally, positioning the spark plug laterally exacerbated performance issues, as it led to heat exchange primarily with the wall before interacting with the air-fuel mixture.

5. ACKNOWLEDGEMENTS

The authors acknowledge the support from to FUNDEP – UFMG Support Foundation – ROTA 2030 coordinator from the research through the project 27192*6 - “Ultra-high pressure injection for flex-fuel engines: technological challenges for ethanol”.

The authors are also grateful for the support provided by CNPq – Brazilian National Council for Scientific and Technological Development – for Mr. Lacava the research grant – process 309690/ 2017-0. To FAPESP – São Paulo Research Foundation (Brazil) - and Stellantis Group for supporting the research through the project 13/50238-3, in the context of the Engineering Research Center Prof. Urbano Ernesto Stumpf.

6. REFERENCES

Aleiferis, P.G. and Behringer, M.K., 2015. “Flame front analysis of ethanol, butanol, iso-octane and gasoline in a spark-ignition engine using laser tomography and integral length scale measurements”. *Combustion and Flame*, Vol. 162, No. 12, pp. 4533–4552.

Aleiferis, P., Serras-Pereira, J. and Richardson, D., 2013. “Characterisation of flame development with ethanol, butanol, iso-octane, gasoline and methane in a direct-injection spark-ignition engine”. *Fuel*, Vol. 109, pp. 256–278.

Aleiferis, P., Serras-Pereira, J., Van Romunde, Z., Caine, J. and Wirth, M., 2010. “Mechanisms of spray formation and combustion from a multi-hole injector with e85 and gasoline”. *Combustion and Flame*, Vol. 157, No. 4, pp. 735–756.

Augoye, A. and Aleiferis, P., 2014. “Characterization of flame development with hydrous and anhydrous ethanol fuels in a spark-ignition engine with direct injection and port injection systems”. Technical report, SAE Technical Paper.

Di Iorio, S., Sementa, P. and Vaglieco, B.M., 2016. “Analysis of combustion of methane and hydrogen–methane blends in small di si (direct injection spark ignition) engine using advanced diagnostics”. *Energy*, Vol. 108, pp. 99–107.

Henrique Rufino, C., Moraes Coraça, E., Teixeira Lacava, P. and Ferreira, J.V., 2023. “Deep learning based techniques for flame identification in optical engines”. *International Journal of Engine Research*, Vol. 24, No. 5, pp. 1877–1891.

Heywood, J.B., 1988. "Internal combustion engine fundamentals".

Irimescu, A., Tornatore, C., Marchitto, L. and Merola, S.S., 2013. "Compression ratio and blow-by rates estimation based on motored pressure trace analysis for an optical spark ignition engine". *Applied Thermal Engineering*, Vol. 61, No. 2, pp. 101–109.

Kim, K., Kim, J., Oh, S., Kim, C. and Lee, Y., 2017. "Evaluation of injection and ignition schemes for the ultra-lean combustion direct-injection lpg engine to control particulate emissions". *Applied Energy*, Vol. 194, pp. 123–135.

Malheiro de Oliveira, E.R., Rufino, C.H. and Lacava, P.T., 2022. "Effects of direct injection and mixture enleament on the combustion of hydrous ethanol and an ethanol-gasoline blend in an optical engine". *Fuel*, Vol. 327, p. 125137.

Martinez, S., Irimescu, A., Merola, S.S., Lacava, P. and Curto-Riso, P., 2017. "Flame front propagation in an optical gdi engine under stoichiometric and lean burn conditions". *Energies*, Vol. 10, No. 9, p. 1337.

Otsu, N., 1979. "A threshold selection method from gray-level histograms". *IEEE transactions on systems, man, and cybernetics*, Vol. 9, No. 1, pp. 62–66.

Ozdor, N., Dulger, M. and Sher, E., 1994. "Cyclic variability in spark ignition engines a literature survey". *SAE transactions*, pp. 1514–1552.

Solferini de Carvalho, F., Peñaranda Mendoza, A., Ribeiro dos Santos, L., Henrique Rufino, C., Malheiro de Oliveira, E., Ferreira Silva, M., Blanco Machin, E., Travieso Pedroso, D. and Teixeira Lacava, P., 2022. "Experimental study of the methane and producer gas blends in an optical spark ignition engine: Combustion characteristics, thermodynamics and emissions". *International Journal of Engine Research*, p. 14680874221131117.

Winklhofer, E., 2001. "Optical access and diagnostic techniques for internal combustion engine development". *Journal of Electronic Imaging*, Vol. 10, No. 3, pp. 588–592.

7. RESPONSIBILITY NOTICE

The authors are solely responsible for the printed material included in this paper.